Journal of Physics and Chemistry of Solids 87 (2015) 244–252

Contents lists available at ScienceDirect

Journal of Physics and Chemistry of Solids

journal homepage: www.elsevier.com/locate/jpcs

Sunlight assisted photodegradation by tin oxide quantum dots

P.S. Shajira, V. Ganeshchandra Prabhu, M. Junaid Bushiri *

Nanofunctional Materials Laboratory, Department of Physics, Cochin University of Science and Technology, Kochi 682022, Kerala, India

A R T I C L E I N F O

Article history:
Received 8 April 2015
Received in revised form
18 July 2015
Accepted 2 September 2015
Available online 8 September 2015

Keywords:
Oxides
Chemical synthesis
Raman spectroscopy
Defects
Luminescence

A B S T R A C T

Rutile phase of SnO_2 quantum dots of average size of 2.5 nm were synthesized at a growth temperature of 70 °C and characterized with XRD, TEM, FTIR and Raman analysis. The effective strain within the lattice of SnO_2 quantum dots was calculated by Williamson–Hall method. The broad peaks in XRD as well as Raman spectra and the presence of Raman bands at 569 and 432 cm^{-1} are due to lower crystallinity of nanoparticles. The optical band gap of SnO_2 quantum dots was increased to 3.75 eV attributed to the quantum size effect. SnO_2 quantum dots were annealed in air atmosphere and the crystallite size of the particles increased with annealing temperature. Sunlight assisted photodegration property of SnO_2 quantum dots was investigated with vanillin as a model system and it shows the photodegradation efficiency of 87%. The photoluminescence and photodegradation efficiency of nanocrystallite SnO_2 decreases with increase of crystallite size contributed to the reduction in population of defects and surface area.

1. Introduction

Tin oxide (SnO_2) is a wide band gap (3.62 eV) semiconducting material at room temperature and has a high exciton binding energy (130 meV) [1]. The applications of tin oxide span over the fields of transparent conducting electrodes, gas sensors, liquid crystal displays, lithium ion batteries, catalyst of chemical reactions, photocatalysis etc. [2–10]. Photocatalysis is an effective and ecofriendly alternative for existing water purification methods. Photocatalytic efficiency is relatively very poor for tin oxide nanoparticles due to small spatial charge separation and comparatively high recombination rate of photogenerated charge carriers [7]. Usually heterophase/heterojunction nanomaterials are used to increase photocatalytic efficiency since the above mentioned problems can be reduced [11]. Since the band gap of commonly used photocatalysts lie in the UV region, they usually utilize UV light source which is relatively expensive. Energy levels of semiconductors can be modified by doping or by using heterojunctions made of semiconductors with different band gaps, thus the absorption in visible region can be enhanced and the solar energy can be utilized for photocatalysis [12,13]. Oxygen vacancies in semiconductors will act as a self dopant, it can modify the energy levels and enhance visible photocatalytic efficiency [14]. Apart from that, the oxygen vacancies present in quantum dots can trap photogenerated electrons and thus to reduce the recombination rate [14]. Vanillin (4-hydroxy-3-methoxy benzaldehyde) is a phenolic aldehyde and can be taken as a model organic compound for water contaminant since it is widely used in food and fragrance industries [15]. Its increased amount in water will affect aquatic organisms like algae and fish [16]. Its acute amount in soil will cause the reduction in germination rate in plants like cotton and also causes death of ecosystem engineers like earthworm [17,18].

The physical, chemical properties and the structure of nanomaterials strongly depend on the preparation methods. SnO_2 nanoparticles can be prepared by combustion, sol gel, microwave, hydrothermal, pulsed laser deposition, solid state reaction and chemical methods [19–25]. Microwave irradiation method is used for the synthesis of SnO_2 nanoparticles of average particle size 2.8 nm with oleyl amine as capping agent [26]. The synthesis of SnO_2 nanoparticles of average particle size 3.5 nm also reported which is by a non-aqueous benzyl alcohol route [27]. A surfactant free hydrothermal method is also exploited for the synthesis of SnO_2 nanoparticles at a temperature of 225 °C which gives particles of average size 5.8 nm [28]. In this regard, quantum dots which may exhibit quantum confinement effect are very important and a simple route of synthesis is necessary for its bulk production. The low reaction temperature is one of the favourable conditions for the growth of quantum dots. In the present study, SnO_2 quantum dots of average crystllite size 2.5 nm were synthesized by a simple ligant/surfactant free chemical precipitation method using eco friendly calcium oxide as reagent at a low temperature of 70 °C for the first time to the best of our knowledge. The optical band gap is determined and its photocatalytic

* Corresponding author.
E-mail address: junaidbushiri@gmail.com (M.J. Bushiri).

http://dx.doi.org/10.1016/j.jpcs.2015.09.003
0022-3697/

efficiency was investigated by using vanillin as a model pollutant in the presence of sunlight. The effect of annealing of SnO_2 nanoparticles in air atmosphere on photodegradation efficiency is also studied.

2. Experimental

2.1. Sample preparation

SnO_2 quantum dots were synthesized by the reaction of 100 ml each of CaO (0.2 M) and $SnCl_4 \cdot 5H_2O$ (0.1 M) aqueous solutions at a temperature of 70 °C for three hours under constant stirring in a reaction flask. The so obtained white precipitate was filtered and washed with ethanol, glycerol and distilled water and the unreacted reagents were removed.

The reactions that may occur during the synthesis of SnO_2 quantum dots can be represented as follows which is similar to that of reaction between Na(OH) and $SnCl_4 \cdot 5H_2O$ reported by Kar et al. [26].

$$2CaO + 2H_2O \rightarrow 2Ca(OH)_2$$

$$2Ca(OH)_2 + SnCl_4 \cdot 5H_2O \rightarrow 2CaCl_2 + Sn(OH)_4 + 5H_2O$$

$$Sn(OH)_4 \rightarrow 2H_2O + SnO_2$$

And the total reaction may be

$$CaO + SnCl_4 \cdot 5H_2O \rightarrow SnO_2 + 2CaCl_2 + 5H_2O$$

The as synthesized SnO_2 sample (SnQ) was annealed at 300 (SnQ300) and 500 °C (SnQ500) in air atmosphere.

2.2. Characterization

The X ray powder diffraction patterns of the samples were recorded using a Rigaku D Max powder X ray diffractometer with Cu-Kα radiation ($\lambda = 1.5414$ Å). The Fourier transform infrared (FTIR) spectra of the samples were obtained by using IRAffinity-1 FTIR spectrophotometer in the range 400–4000 cm^{-1} by KBr pellet technique. A Horiba Jobin Yvon Lab Ram HR system with Ar-ion laser (514.5 nm) as the excitation source (resolution 3 cm^{-1}) was used for Raman measurements in the Stokes region. The selected area electron diffraction (SAED) and high resolution transmission electron microscopy (HRTEM) of the sample (SnQ) were obtained from JOEL JEM 2100 operated at 200 keV. UV–vis reflection spectra of SnO_2 nanoparticles were recorded in diffuse reflectance mode (DRS) with JASCO V-570 UV–vis spectrophotometer in the range 190–800 nm for the powder samples using $BaSO_4$ as reference. The photoluminescence (PL) measurement was carried out with Lab-RAM HR 800 spectrometer by using He–Cd laser ($\lambda = 325$ nm) as excitation source at room temperature. UV–vis absorption spectra of photocatalytically degraded solution were studied by using JASCO V-570 UV–vis spectrophotometer.

3. Results and discussion

3.1. Structural characterization by XRD

XRD pattern of the as synthesized samples reveal the formation of the tetragonal rutile phase of SnO_2 which can be indexed to JCPDS no. 41-1445 (Fig. 1). The prominent diffraction peaks are obtained from the sample SnQ at 2θ values 26.3, 33.1 and 51.4° corresponds to (110), (101) and (211) planes respectively. The diffraction peaks from (221), (112) and (301) are overlapped

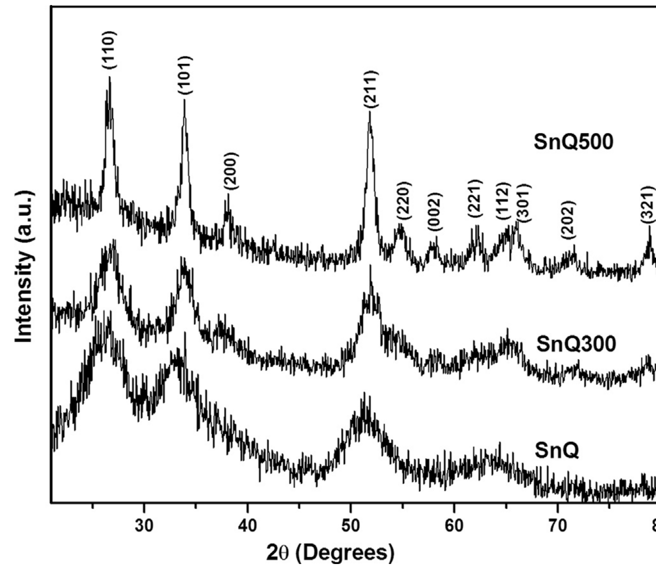

Fig. 1. XRD patterns of SnO_2 quantum dots (SnQ) synthesized by chemical reaction at a temperature of 70 °C and the samples annealed at 300 (SnQ300) and 500 °C (SnQ500).

together due to the broadness of peaks and observed at 2θ value 63.4°. The broadening of the diffraction peaks shows that obtained particles are in nanoregime and the average crystallite size of the sample calculated by Scherrer's formula is about 2.5 nm [29]. For annealed SnO_2 samples at 300 and 500 °C (SnQ300 and SnQ500), the XRD peaks become sharper with increase in annealing temperature indicating the increase in crystallite size. The obtained crystallite sizes of SnQ300 and SnQ500 are 5 and 12 nm respectively calculated by Scherrer's formula. The broad XRD peak observed at 63.4° is resolved upon annealing of SnQ at a temperature of 500 °C and appeared at 62.3, 64.7 and 65.9° corresponds to (221), (112) and (301) respectively due to the increase in crystallinity of the samples. Lattice parameters are calculated from (110) and (101) planes and are given in Table 1 [30]. The slight increase in lattice parameters than the value reported in JCPDS in SnQ sample probably due to the modification in Sn–O bonds by hydroxyls adsorbed on SnO_2 crystallite surfaces [31].

To calculate the effective strain within the lattice Williamson–Hall plots (W–H plots) of SnQ, SnQ300 and SnQ500 samples were drawn (Fig. 2). According to Williamson–Hall equation the strain can be obtained from the slope and the crystallite size is measured from the intercept value of the plot between $\beta\cos\theta/\lambda$ and $\sin\theta/\lambda$ [32]. The strain values and crystalline sizes obtained are given in Table 1. Slope of W–H plot of SnQ is positive having a strain of 3.01% while SnQ300 shows a small compressive strain of −1.7%. However for SnQ500 sample a positive slope is obtained which reveals that there is a resultant tensile strain in the sample. The average crystallite size obtained from the intercept values of linear

Table 1
Structural parameters and band gap of SnO_2 and annealed SnO_2 nanoparicles synthesized by chemical method.

Sample	Lattice parameters (Å)		Cell volume (Å^3)	Crystallite size (nm)		Strain	Band gap (eV)
	a	*c*		From Scherrer's formula	From W–H plot		
SnQ	4.7962	3.2886	75.65	2.5	3.18	3.01	3.75
SnQ300	4.7314	3.1932	71.48	5	4.6	−1.7	3.14
SnQ500	4.7338	3.1889	71.46	12	10.8	8	2.8